Yu-Shiba-Rusinov states of a single magnetic molecule in an *s*-wave superconductor

Saurabh Pradhan and Jonas Fransson
Department of Physics and Astronomy, Box 516, Uppsala University, Uppsala 75120, Sweden

(Received 31 January 2020; revised 6 August 2020; accepted 6 August 2020; published 19 August 2020)

We use the numerical renormalization group theory to investigate the Yu-Shiba-Rusinov (YSR) bound state properties of single magnetic molecules placed on an *s*-wave superconducting substrate. The molecule is modeled as a large core spin and a single orbital, coupled via exchange interaction. The critical Coulomb interaction for the singlet/doublet transition decreases in the presence of this exchange interaction for both ferro- and antiferromagnetic couplings. The number of YSR states also increases to two pairs; however, in the singlet phase, one of the pairs has zero spectral weight. We explore the evolution of the in-gap states using the Anderson model. Away from the particle-hole symmetry point, the results suggest a doublet-singlet-doublet transition as the on-site energy is lowered while keeping the Coulomb interaction fixed. We construct an effective model for the molecule to understand these results, in the limit of the large superconducting order parameter. Qualitatively, the model accounts for the phase transitions and spectral nature of the in-gap states. Finally, we analyze the effects of magnetic anisotropic fields of the core spin on in-gap states. Due to internal degrees of freedom of the spin excited states, a multitude of new states emerges within the gap. Depending on the sign and strength of the uniaxial anisotropic field, the results indicate up to three pairs of YSR states.

DOI: 10.1103/PhysRevB.102.085136

I. INTRODUCTION

Nanoscale devices embedded in tunnel junctions provide unique opportunities to study quantum many-body effects of impurity systems. In recent years, there have been tremendous advancements over the control of such devices, where the number of electrons is electrostatically controlled in a small restricted region. Whenever these devices contain an odd number of electrons, the Kondo effect [1–3] arises due to multiple spin-flip scattering processes. Quantum dots [4,5], magnetic adatoms [6–8], and magnetic molecules [9–11] are examples of microscopic systems that display the Kondo effect when mounted between metallic electrodes.

Low-temperature experiments with localized magnetic moments adsorbed onto a superconducting surface display the emergence of bound states inside the superconducting gap [12]. This was first measured using scanning tunneling microscopy and spectroscopy [13] for single magnetic impurities, which has subsequently been reproduced under different experimental conditions, such as a magnetic field [14,15]. Understanding the detailed dynamics of the smallest possible magnetic systems is important for fundamental reasons since it provides insight into the mechanisms that govern the physics of magnetic moments interacting with superconducting materials. Magnetic impurities can hold Majorana modes [16] in a superconducting substrate [17]. Theoretically, the emergence of in-gap bound states was predicted by Yu [18], Shiba [19], and Rusinov [20] using semiclassical approaches where, specifically, the spin moment was treated as classical. Quantum effects of magnetic impurities were later studied within mean-field theory [21–23], perturbation theory [24,25], and numerical renormalization group (NRG) theory [26–31].

The ground state of a quantum magnetic impurity in a metal substrate is a Kondo singlet with a characteristic energy scale related to the Kondo temperature (T_k). However, in a superconductor, the substrate electrons form Cooper pairs, which are not compatible with the Kondo singlet state. The fundamental interactions associated with the superconducting gap (Δ_{sc}) and the Kondo temperature compete, and at large Δ_{sc} the ground state becomes a doublet formed by the substrate and impurity electron states. The ratio of the two energy scales determines the nature of the ground state as well as the energies of the bound states inside the gap. The bound state energy coincides with the energy of the edge of the superconducting gap for weak coupling between the spin moment and the surface states, and they move inside the gap for increasing coupling strength, eventually crossing the Fermi energy when the two energy scales are similar, $T_k \approx \Delta_{sc}$.

The bound states always come in pairs of particle-hole symmetric states around the Fermi energy. Recently, more than one pair of Yu-Shiba-Rusinov (YSR) states were observed [32,33] in experiments with magnetic molecules. Multiple pairs of YSR states have been attributed to the presence of many orbitals in the molecule. The coupling of these orbitals with the substrate is not uniform due to the different nature of the orbitals. As a result, the energies of the YSR states of the different orbitals may have different energies

and weights. Results from NRG calculations of large spin moments with magnetic anisotropy show that multiple pairs of YSR states may appear [34] due to internal spin excitation. These calculations, however, do not take into account differences due to the localized and delocalized nature of the d and the ligand orbitals, respectively.

Here, we have considered an Anderson impurity model in which superconducting surface states play the role of the reservoir electrons coupled with a core spin. Due to the presence of the core spin, multiple YSR states emerge inside the superconducting gap. This model naturally reflects the geometry of large spin molecular systems such as Fe_8 [35], Mn_{12} [36], and transition-metal phthalocyanines [32,37]. The ligand orbitals of the molecule form degenerate orbitals that couple with the surface electrons in the substrate. For simplicity, we have considered a single-orbital Anderson impurity model for the ligand orbitals. This orbital represents the lowest unoccupied molecular orbital (LUMO), since this is the most important orbital in the vicinity of the Fermi level. Here we consider only one molecular orbital, as our calculation becomes very expensive with a number of molecular orbitals. The d-orbital electrons of the transition-metal atom have a negligible hybridization with the ligand orbitals and, therefore, form a local magnetic moment. We have assumed that the spin moment of the transition-metal atom interacts only with electrons in the ligand orbital via exchange and has no interaction with the substrate electrons. This is because the energies of the d-orbital states are far below the Fermi level, which tends to suppress the charge fluctuations. The unpaired electrons of these orbitals only give a magnetic moment. In other words, the large Coulomb interaction of the d-orbital forbids double occupancy, and spins are exchange coupled with a molecular orbital. As a result, the spins of the metal atom do not interact directly with the substrate. We have considered the magnetic moment of the transition-metal atom to be large ($S > 1/2$). Due to the spin-orbit coupling and spatial structure of the substrate, we have also included magnetic anisotropy for the core spin. In the case of phthalocyanine molecules, some d-orbitals can form a core-spin without hybridizing with the substrate while other d-orbitals do hybridize. The latter scenario does give rise to a pronounced Kondo effect [38].

This paper is organized as follows. In Sec. II, the model is defined and we present a brief description of the NRG method. In Sec. III, we derive an effective model for our system in the limit of a large superconducting gap. This gives a better understanding of the NRG results and qualitatively explains various properties of the YSR states. In Sec. IV, we present the NRG results. In Sec. IV A, we discuss the proximity-induced superconducting order parameter in the molecule, whereas in Sec. IV B we discuss the behavior of the YSR state as a function of the Coulomb interaction for different values of the exchange interaction. Then we discuss the spectral weight of the YSR states. The single-particle transition from the ground state is only possible when the spectral weight is nonzero. In Sec. IV C, we change the on-site energy of the orbital away from the particle-hole symmetric point, while in Sec. IV D, finally, we look at the behavior of the YSR as we turn on the magnetic anisotropy field. The paper is concluded and summarized in Sec. V.

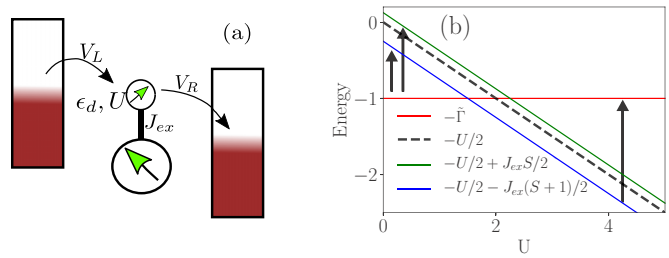

FIG. 1. (a) Schematic diagram of the magnetic molecule in a tunnel junction with tunneling strengths ($V_{L,R}$). ϵ_d, U, and $J_{\rm ex}$ are the on-site, Coulomb, and exchange energy of the molecule. (b) Energy eigenvalues of the effective Hamiltonian as a function of Coulomb energy (U) in the large Δ limit. The arrow indicates the possible single-particle transition from the ground state.

II. MODEL AND METHODS

We consider the magnetic molecule to be embedded in a tunnel junction between metallic electrodes, as depicted in Fig. 1(a). We have considered V_L to be very small and only measure the properties of the molecule. As a result, we consider our system to consist of the molecule and the right lead with coupling $V = V_R$. The total Hamiltonian of the system is given by

$$H = H_{\rm mol} + H_{\rm sc} + H_{\rm T}, \tag{1a}$$

$$H_{\rm mol} = \epsilon_d n_d + U n_\uparrow n_\downarrow + J_{\rm ex}\mathbf{s}\cdot\mathbf{S} + H_{\rm S}, \tag{1b}$$

$$H_{\rm S} = DS_z^2, \tag{1c}$$

$$H_{\rm sc} = \sum_{k\sigma}\epsilon_k c_{k\sigma}^\dagger c_{k\sigma} - \Delta_{\rm sc}\sum_k (c_{k\uparrow}^\dagger c_{-k\downarrow}^\dagger + {\rm H.c.}), \tag{1d}$$

$$H_{\rm T} = \sum_{k\sigma} V_k (c_{k\sigma}^\dagger d_\sigma + {\rm H.c.}). \tag{1e}$$

The molecule consists of a single orbital labeled with the on-site energy ϵ_d and Coulomb repulsion energy U, $n_\sigma = d_\sigma^\dagger d_\sigma$ is the number operator for each spin, $d_\sigma^\dagger$ is the creation operator for the orbital, and $n_d = n_\uparrow + n_\downarrow$ is the electron occupation number of the orbital. The orbital spin ($\mathbf{s}$) and the core spin ($\mathbf{S}$) interact via exchange interaction ($J_{\rm ex}$). To describe magnetic molecules in general, we have included an anisotropy field (D) for the core spin. For simplicity, here we have not included the transverse anisotropic term $E(S_x^2 - S_y^2)$. The electrons in the superconducting substrate are described by the s-wave Bardeen-Schrieffer-Cooper (BCS) mean-field Hamiltonian ($H_{\rm sc}$). The first term of $H_{\rm sc}$ describes the kinetic energy part of the free electrons in the substrate. In the absence of superconductivity, we assumed that the substrate has a constant density of electron states, $\rho_0 = 1/2\mathcal{D}$, within $[-\mathcal{D}, \mathcal{D}]$ with a bandwidth $2\mathcal{D}$. Henceforth, we take $\mathcal{D}$ as the absolute energy scale of the system and set it to be $\mathcal{D} = 1$. We have added a BCS order parameter $\Delta_{\rm sc}$, and the temperature dependence of the $\Delta_{\rm sc}$ is neglected, as we only discuss the ground-state properties. Here, we have neglected electron-electron interactions in the substrate. We also fix $\Delta_{\rm sc}/\mathcal{D} = 2 \times 10^{-4}$ and $S = 2$.

In this work we use NRG theory [27,39–44], which is an unbiased nonperturbative method that works perfectly at

both zero and finite temperatures. First, we discretize the noninteracting substrate electrons such that the electrons are described by a finite number of states, logarithmically separated from each other. Second, we transform this system into a linear chain that begins with the molecule. The on-site energy of the linear chain becomes zero for reservoir electrons, with a particle-hole symmetric density of states, whereas the hopping elements decrease exponentially with increasing distance away from the molecule. We use the NRG discretization parameter $\Lambda = 2.5$ throughout this paper.

The exponential decrease of the energy scale of successive sites in the linear chain ensures the success of the NRG method for the metallic substrate. For the superconducting substrate it was initially thought, however, that the superconducting gap Δ_{sc} would cause a problem for the NRG iteration, since the argument of energy scale separation no longer holds for large Wilson chains. In other words, the perturbation of adding a site to the Wilson chain is no longer sufficiently small to allow truncating the NRG iteration at site N where $\Lambda^{-N/2}$ is comparable to Δ_{sc} [39,40]. It was nevertheless pointed out that the energy scale separation of NRG works even beyond this value of N, and that the perturbations become even smaller with finite Δ_{sc} [42]. Hence, in the presence of superconductivity, the NRG approximation becomes even more accurate.

III. LARGE Δ LIMIT

Before discussing the NRG results, we consider a simplified version of the model in Eq. (1), obtained in the limit of large Δ_{sc}, to gain some understanding of the expected behavior of the many-body YSR bound states. As is illustrated for the single-orbital Anderson model in Refs. [45,46], the substrate induces superconducting order in the quantum dot when the superconducting gap is the largest energy scale compared to any other energy scales of the system. In this limit, the self-energy, due to the bath electrons, gives only finite off-diagonal components in the Bogoliubov–de Gennes basis for energies much smaller than the superconducting gap. As a result, we can write an effective Hamiltonian for the system. This procedure can also be applied to the molecular system, and the effective low-energy Hamiltonian can be written as

$$H_{\text{eff}} = \epsilon_d n + U n_\uparrow n_\downarrow + \tilde{\Gamma}(d_\uparrow d_\downarrow + \text{H.c.}) + J_{\text{ex}} \mathbf{s}\cdot\mathbf{S}, \qquad (2)$$

where $\tilde{\Gamma}$ is the induced superconducting order in the molecule.

Here we will consider the symmetric Anderson model ($\epsilon_d = -U/2$). In the absence of the exchange term between the orbital spin and the core spin, the ground-state behavior changes as function of U at $U/2 = \tilde{\Gamma}$. The ground state is a doublet state (the antisymmetric combination of $|0\rangle$ and $|\uparrow\downarrow\rangle$) for small U, while for large U the ground state is a singly occupied state. The transition between these two states occurs at $U = 2\tilde{\Gamma}$. The ground-state degeneracy also changes from one to two electrons across this transition, resulting in the expectation values of various operators changing discontinuously.

The energy difference between the ground and first excited states mimics the behavior of the YSR bound states when Δ_{sc} is comparable to the other energy scales in the system. Within this effective model, we can see that the bound state energy

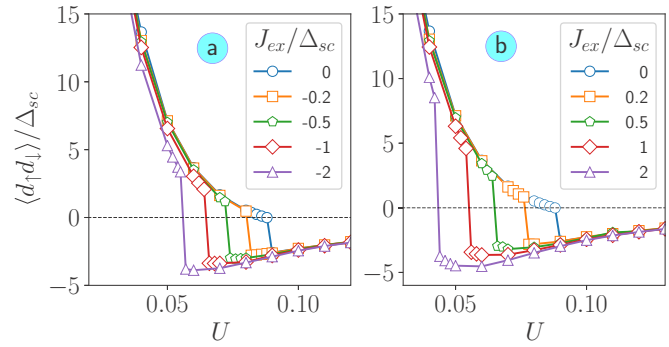

FIG. 2. The expectation value of superconducting order of the orbital label at zero temperature for different values of the Coulomb interaction at fixed values of the exchange interaction $J_{\text{ex}}/\Delta_{sc} \leqslant 0$ (a), $J_{\text{ex}}/\Delta_{sc} \geqslant 0$ (b).

first decreases with increasing U and approaches zero at the transition point, while it increases again after the transition point; see Fig. 1(b).

In the presence of finite exchange interaction between the orbital spin and core spin, the doublet ground state remains unaffected while the degeneracy of the singly occupied state is lifted. The energies of the singly occupied states are now $-U/2 + J_{\text{ex}}S/2$ and $-U/2 - J_{\text{ex}}(S+1)/2$. In Fig. 1(b), the energies of the effective Hamiltonian are plotted as a function of U. The first excited state is split below a critical energy U_c, whereas the ground state splits at a larger U. Even though there are more states within the gap, not all states are visible in the single-particle spectrum at zero temperature. This is clear since for $U < U_c$, transitions between the singly occupied state to both doublet states are possible, while for $U > U_c$, only transitions from the doublet state with the lowest energy to the singly occupied state are allowed, given that the temperature is sufficiently low to prevent thermal excitations of the second doublet state. The arrows in Fig. 1(b) indicate all possible transitions. As a result, a single pair of YSR states emerges in the singlet phase, while two pairs of YSR states should be observed in the doublet phase. We also observe that U_c is shifted toward the lower value for both positive and negative values of the exchange interaction. This can be understood from the fact that the exchange interaction always lowers the energy of the singly occupied state. As mentioned earlier, the energies of the singly occupied states are $-U/2 + J_{\text{ex}}S/2$ and $-U/2 - J_{\text{ex}}(S+1)/2$. One of these states will certainly have lower energy compared to $-U/2$ depending on the sign of J_{ex}.

IV. NRG RESULTS

A. Induced superconductivity

Due to proximity, the superconductor induces a finite pairing potential, or a superconducting order parameter in the molecule. In Fig. 2 we show the expectation values of the induced order parameter as a function of the Coulomb interaction. First, consider the case of vanishing exchange interaction, $J_{\text{ex}} = 0$ (blue circle). It can be clearly seen that the largest values of the order parameter are reached in the noninteracting limit, $U \to 0$, and they decrease with

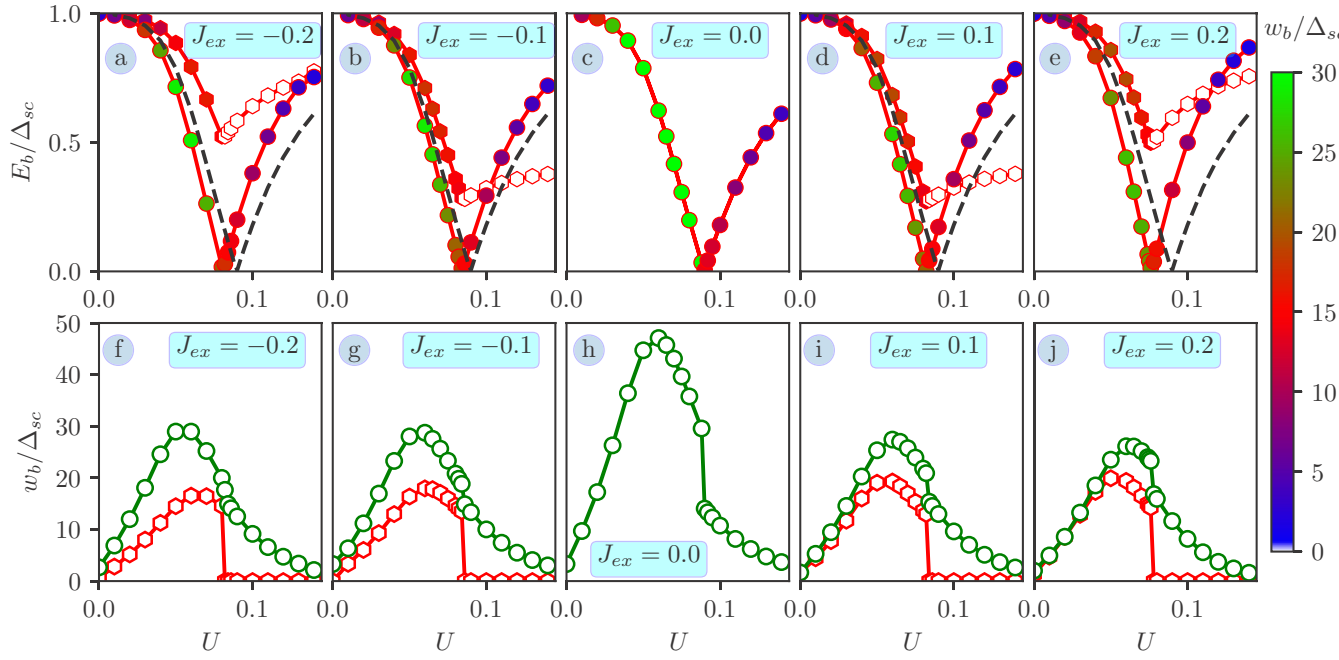

FIG. 3. Bound state energies (a)–(e) and their spectral weight (f)–(j) of the in-gap states for different values of the Coulomb interaction at fixed exchange interaction $J_{ex}/\Delta_{sc} = -0.5$ (a,f), -0.2 (b,g), 0 (c,h), 0.2 (d,i), and 0.5 (e,j). The spectral weights of all of the states are also color-coded. The dashed line indicates the YSR states for $J_{ex} = 0$.

increasing interaction strength U. This can be explained as an effect of the fact that the doubly occupied (and empty state for the symmetric Anderson model) state is less favorable for large U. Since the BCS states are a combination of the empty and doubly occupied states, the induced superconducting order becomes suppressed as the Coulomb interactions become increasingly influential.

A further increase of the Coulomb interaction strength, U, leads to the superconducting order parameter changing sign at the critical interaction energy U_c. At this transition point, the ground state of the molecule changes from a doublet ($U < U_c$) to a singlet ($U > U_c$) state. The discontinuity of the induced order parameter at $U = U_c$ reflects the change in the degeneracy of the ground state when it undergoes a transition from a doublet to a singlet state. In the context of the Josephson junction, this discontinuity is related to the *so-called* 0-π transition. One important thing to notice is that for Coulomb interactions that are weaker than the critical energy U_c, the induced superconducting order has the same phase as the substrate, whereas it is phase-shifted by π in the large-U limit. While the order parameter remains negative for $U > U_c$, its magnitude decreases.

Next, we include a finite exchange interaction, $J_{ex} \neq 0$. Previously, in the bound state analysis of the effective model, Eq. (2), it was shown that the critical energy U_c decreases in the presence of a finite exchange interaction, irrespective of being ferro- and antiferromagnetic. Here, our numerical results corroborate this conclusion, which can be seen in Fig. 2. Specifically, the sign change of the induced superconducting order parameter shifts to a lower U for increasing $|J_{ex}|$. The value of U_c reduces much faster in the case of positive exchange interaction compared to the negative value of the exchange interaction. The core spin (S) and the orbital spin ($s = 1/2$) have eigenstates that can be categorized as a triplet and a singlet, with corresponding energies $J_{ex}S/2$ and $-J_{ex}(S+1)/2$, respectively, in the absence of the substrate. From this, it is evident that the ground-state energy decreases faster when J_{ex} is positive. This makes the reduction in U_c larger when $J_{ex} > 0$. Near the transition point, $U \simeq U_c$, the induced superconducting order parameter is strongly renormalized by the finite exchange interaction. The absolute value of the order parameter is reduced compared to the case when J_{ex} is zero.

B. Bound states and spectral weights

The dimensions of the Hilbert space of the Wilson chain increases by a factor of 4 for each added site. Therefore, we discard higher energy states after a few iterations to keep the size of the Hamiltonian manageable. The maximum number of states that we retain is of the order of 5000. After a sufficient number of NRG iterations ($N = 40$), we obtain all pertinent many-body states. This includes a continuum of states above the superconducting gap and few states below. The states within the superconducting gap are known as Andreev [17], YSR states [18–20], and we shall use the latter nomenclature for the remainder of this article. In Figs. 3(a)–3(e), the YSR states are plotted as a function of the Coulomb energy U of the molecule level for various values of the exchange interaction J_{ex}. Here, the on-site energy of the molecule is $\epsilon_d = -U/2$, which is the symmetric Anderson model. In this case, the single-particle spectrum of the system is particle-hole-symmetric. There exists a negative energy YSR state for each positive energy YSR state (not shown in this figure). By turning off the exchange interaction, that is, setting $J_{ex} = 0$, the model is reduced to an Anderson model with a superconducting reservoir. The associated positive

energy YSR state for this case is shown in Fig. 3(c). It can be seen that there is only one bound state, as expected under degenerate conditions, emerging near the edge of the superconducting gap for small values of U. The doublet state is the ground state and the singlet state becomes the first excited state for lower Coulomb energy. With increasing U, the bound state shifts into the gap, coinciding with the Fermi level ($E_b - E_F = 0$) at the critical energy $U = U_c$. The ground state of the molecule changes from a doublet to a singlet state at this critical energy (U_c). For Coulomb repulsion energies $U > U_c$, the bound state energy shifts away from the Fermi level. At larger U, the singlet state is the ground state and the doublet state is the first excited state. In the metallic system, the Kondo temperature is the only energy scale of the system and the ground state is the Kondo singlet state. By contrast, in the presence of superconductivity, Δ_{sc} becomes a second energy scale of the system. The BCS state of the superconductor and Kondo singlet state compete, giving rise to the singlet to doublet transition.

In our previous discussion of the effective model, Eq. (2), we argued that a large superconducting order parameter ($\Delta_{sc} \to \infty$), accompanied by a finite exchange interaction (J_{ex}), splits the singly occupied states. The result is also valid for finite Δ_{sc}, however it is slightly modified to involve a lifting of the $(2S + 1)$-fold degeneracy of the Kondo singlet. This $(2S + 1)$-fold degeneracy originates from the core spin ($\mathbf{S}$) in the absence of the interaction between the core spin and the molecular orbital. Due to internal spin excitations in the presence of the exchange iteration, new states emerge within the superconducting gap, as shown in Fig. 3. Due to finite exchange interaction, three low-energy states arise (one doublet state and two singlet states). At zero temperature, one of these states becomes the ground state whereas the two other states become higher energy excited states. These two higher energy states are the two YSR states that appear in the positive part of the spectrum, both for positive and negative values of J_{ex}. These two states arise from transitions between the doublet and singlet states; see Fig. 1(b). One of the bound state energies coincides with the Fermi energy at the critical Coulomb energy $U = U_c$. One important thing to notice here is that U_c always reduces, both for ferromagnetic and antiferromagnetic exchange interaction. The energy of the second bound state remains finite for all values of U. The energy of this bound state first decreases with U, has a minimum at $U = U_c$, and increases again for increasing U. This state appears because of the transition from the doublet states to a higher energy singlet state for $U < U_c$. For $U > U_c$, however, the YSR state emerges from singlet to singlet transitions. The energy of this YSR state is indicated as filled and empty hexagons in Figs. 3(a), 3(b), 3(d), and 3(e), respectively. The energy difference between the two singlet states increases with the absolute value of J_{ex}. As a result, the energy of this YSR state (empty hexagon) steadily increases with $|J_{ex}|$ for $U > U_c$. With large enough $|J_{ex}|$ compared to Δ_{sc}, this bound state merges with the continuum states above the superconducting gap.

Next, we make a connection with experiments through a discussion of the single-particle spectrum of the system. This can be measured in experiments, for instance using scanning tunneling microscopy. The conductance thus measured is proportional to the local density of electron states of the single orbital. In the zero-temperature limit, the local density of electron states contains two contributions, one from the states within the superconducting gap and the other from the states outside the superconducting gap. Formally, the local density of states can be written $A(\omega) = A_1(|\omega| < \Delta_{sc}) + A_2(|\omega| > \Delta_{sc})$, $A_1(\omega) = \sum_i w_b^i \delta(\omega - E_b^i)$. In this article, we are only interested in the in-gap part of the spectrum (A_1), and we will not discuss the continuum part of the spectrum (A_2). The operator d_σ is updated after each NRG iteration, and we extract the matrix elements between the ground state and excited state within the SC gap after NRG iterations are finished. This square of this matrix element gives the spectral weight (w_b^i).

The spectral weights and corresponding energies of the in-gap states are plotted in Fig. 3 for both positive and negative values of the exchange interaction J_{ex}. Here, the on-site energy of the orbital is $\epsilon_d = -U/2$, which is the symmetric Anderson model, imposing particle-hole symmetry in the spectrum such that the bound states with positive and negative energies have equal weights. Previously, it has been shown that the spectral weight is discontinuous at $U = U_c$ [27]. Due to the presence of the exchange interaction, two YSR states with finite weight arise in the spectrum for $U < U_c$, which is consistent with the large Δ_{sc} model (see the arrows in Fig. 1 for smaller U). The two bound states arise from transitions between the doublet ground state and the two singlet states. These two YSR states reduce to one when J_{ex} is zero. It can be seen that both weights increase with U, and that the weight of the state with the higher energy drops to zero at $U = U_c$, as indicated by empty symbols in Fig. 3. The weight of the other state shows a discontinuity at $U = U_c$. The size of the jump at the discontinuity depends on the sign of the exchange interaction J_{ex}, which appears more prominently for antiferromagnetic exchange interaction. To the right of the transition point, that is, $U > U_c$, the spectral weights gradually decrease with increasing U. The zero of spectral weight can be explained from the symmetry arguments. The presence of superconductivity breaks the charge symmetry of the problem, but the spin is still a converse quantity. We can use S_z of the total system to characterize the different many-body states of the system including the ground state [34]. The single-particle transitions from the ground state to a higher energy state should have a difference of S_z that is $1/2$. These transitions gave rise to the YSR states. If the difference of S_z between a ground state and an excited state is not equal to $1/2$, then the spectral weight of those states will be zero.

We summarize the discussion of the single-particle spectrum by noting that below the critical point, $U < U_c$, two pairs of YSR states emerge in the superconducting gap whereas only one pair is observed above, $U > U_c$. This is one important result of this article. In the molecular setup, it should be possible to vary the ratio U/Γ, and we expect that such variations should enable observations of transitions between two pairs and one pair of YSR states.

C. Away from particle-hole symmetry

Even though the symmetric Anderson model is most often used in the existing theoretical literature, such asymmetry is

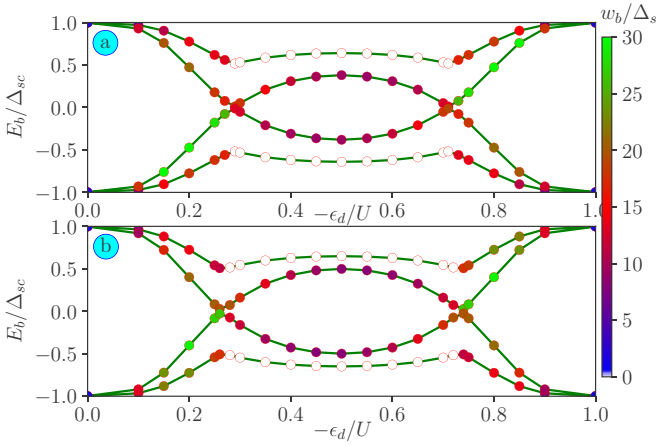

FIG. 4. Bound state energies of the molecule for different value of on-site energy of the orbital away from the particle-hole symmetric point for both ferromagnetic $J_{ex} = -0.2$ (a) and antiferromagnetic $J_{ex} = 0.2$ (b) at a fixed $U = 0.10$.

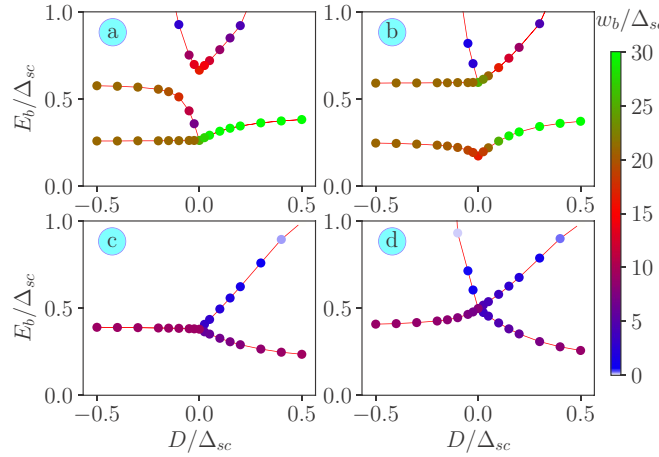

FIG. 5. Bound state energies and the color-coded spectral weights of the molecule for different values of an anisotropic field for $U = 0.07$ (a,b), 0.10 (c,d), $J_{ex}/\Delta_{sc} = -0.2$ (a,c), 0.2 (b,d). Here we have only shown the states with finite spectral weight.

most likely not present in a realistic experimental setup. Apart from this, it is also possible to effectively shift the on-site energy by applying a gate voltage to the system. Thus motivated, we change the on-site energy of the molecular orbital from the symmetric value, noticing that the particle-hole symmetry is removed for $\epsilon_d \neq -U/2$. Therefore, we cannot expect the positive and negative half of the spectrum to be symmetric. In Fig. 4, we plot the energies and spectral weights of the YSR bound states both for positive and negative energies. Here, the Coulomb interaction is fixed at $U = 0.10$ while varying the on-site energy of the orbital for both ferromagnetic [Fig. 4(a)] and antiferromagnetic [Fig. 4(b)] exchange interactions. It can be noticed that for both ferromagnetic and antiferromagnetic exchange interactions, the molecular ground state remains in the doublet regime for small negative on-site energy, which leads to the emergence of two pairs of YSR states. While the YSR states in the doublet phase coincide with the edges of the superconducting gap at $\epsilon/U = 0$, they are shifted inside the gap with increasing $-\epsilon_d/U$, and eventually transition into the singlet phase where only a single pair of YSR states with finite weight exists. We have chosen the Coulomb interaction in such a way that at the symmetric points ($\epsilon_d = -U/2$) we are in the singlet phase. With a further increase of $-\epsilon_d/U$, the system reenters the doublet phase where two YSR states reappear. This reentrance of the phases can be attributed to the nonlinear behavior of the doublet ground-state energy as a function of on-site energy, and it can be understood in terms of the large Δ_{sc} effective model. The energies of the effective model, Eq. (2), in the absence of the exchange interaction are ϵ_d and $\epsilon_d + U/2 \pm \sqrt{\tilde{\Gamma}^2 + (\epsilon_d + U/2)^2}$. While the former energy refers to the singlet state, depending linearly on ϵ_d, the latter energies refer to the doublet states, depending nonlinearly on ϵ_d. From this observation, it is evident that the system is in the doublet phase for small ϵ_d and in the singlet phase for intermediate values of ϵ_d. It is also possible to always remain in the doublet phase by varying U and $\tilde{\Gamma}$ such that the ratio $U/\tilde{\Gamma}$ remains nearly unchanged.

D. Effect of the anisotropy field

Large spin molecules are always subject to more or less strong anisotropic fields due to spatial structure and the intrinsic spin-orbit coupling of the substrate. To describe a physical molecular system, we add a uniaxial anisotropy term to the core-spin Hamiltonian, that is, $H_S = DS_z^2$. The anisotropy field lifts the degeneracy of the singlet and doublet states, creating possibilities for the emergence of additional YSR states inside the superconducting gap. We also notice that positive (negative) values of the parameter D refer to uniaxial anisotropies, which, respectively, lead to a low- (high-) spin ground state. In Fig. 5, we plot the evolution of the YSR states for various combinations of the Coulomb and exchange interactions. We have chosen $U = 0.07$ and 0.10, such that the ground state is in the doublet and singlet phase, respectively, both for ferromagnetic and antiferromagnetic exchange interactions. In the presence of exchange interaction and an anisotropic field, many more states appear within the gap. But not all of them have nonzero single-particle spectral weight. The states with zero spectral weight are not shown in the figures.

First, consider the lower Coulomb interaction, $U = 0.07$ [Figs. 5(a) and 5(b)]. For ferromagnetic interaction [Fig. 5(a)], the two YSR states of the doublet phase evolve into three distinct YSR states for small negative values of the anisotropy field D. For larger negative values of anisotropy parameter D, however, one of these YSR states merges into the edge of the superconducting gap, while the energies of the two remaining YSR states remain almost constant. On the other hand, for small positive values of the anisotropy parameter D, two YSR states appear out of which one merges into the edge of the superconducting gap as D increases. By contrast, for antiferromagnetic exchange interaction the picture changes, which can be viewed in Fig. 5(b) ($U = 0.07$ and $J_{ex} = 0.2$). At this value of U, the ground state is still in the doublet phase, and in the absence of an anisotropic field we see two YSR states. The higher-energy YSR state splits into two YSR states for negative D, while it remains as a single YSR state

for positive D. As was shown in Fig. 5(b), one of the YSR states merges into the continuum states above Δ_{sc} with an increasing value of $|D|$. However, at $D = 0$ the lower-energy YSR state does not split, and its energy increases and saturates for increasing $|D|$. As a result, two YSR states for negative values of D and one YSR state are visible in the positive half of the spectrum.

Next we consider the case for larger Coulomb energy at $U = 0.10$ in Figs. 5(c) and 5(d). We are now in the singlet phase, and only one YSR state appears with finite weight at $D = 0$. We have shown the evolution of YSR states for negative values of J_{ex} in Fig. 5(c). Here, a single YSR state at $D = 0$ remains as a single YSR state for negative values of D while it splits into two YSR states for positive values of D. The energy difference between these two increases with D. The YSR states of the molecule are shown in Fig. 5(d) for a positive value of exchange interaction ($J_{ex}/\Delta_{sc} = 0.20$). Here, a single YSR state at $D = 0$ splits into two YSR states for both positive and negative values of the anisotropic field.

To summarize the effect of the anisotropic field, we see huge changes in the YSR states. The number of YSR states increases due to internal spin excitations of the molecular core spin for small values of the anisotropic field. With larger values of the anisotropic field, some of the YSR state energies move to higher energies and end up mixed up with the continuum of states above the superconducting gap. Depending on the various experimental conditions and spatial structure of the molecule and substrate, the actual values of U/Γ, J_{ex}, and D can be different. As a result, the number of visible YSR states in a scanning tunneling microscopy experiment can be different even for the same molecule.

V. SUMMARY AND CONCLUSION

In conclusion, we have considered the properties of YSR states created from a magnetic molecule absorbed on the surface of an s-wave superconductor. The molecule is modeled as a single orbital and a core spin, coupled via an exchange interaction. The competition between the Kondo effect and superconductivity determines the nature of the many-body ground state and the excited states of the molecule-superconductor complex. Depending on the ratio between the energy scales associated with the Kondo effect and superconductivity, the ground state of the emerging YSR states can be either a singlet or a doublet. The induced superconducting order parameters on the molecule show a discontinuity and change sign at the singlet-doublet transition point, related to the different ground degeneracies of the singlet and doublet states. The exchange interaction is a crucial ingredient of our system as it lifts the degeneracy of the singlet state. As a result, two pairs of YSR states appear. In general, however, in the singlet phase only one of the pairs has finite spectral weight at zero temperature. These results based on NRG simulations are qualitatively consistent with analytical predictions made for large Δ_{sc} in terms of the effective model given in Eq. (2).

Furthermore, we studied the effects of the on-site energy in a setup out of the particle-hole symmetry point ($\epsilon_d = -U/2$). Here, the Coulomb interaction is fixed such that the ground state retains the singlet phase with one pair of YSR states at the particle-hole symmetric point. At a critical point, the system undergoes a transition into a doublet state ground state as the on-site single electron energy ϵ_d is either increased or decreased. One of the YSR states approaches the Fermi energy at the transition point. This effect is predicted to be measurable in experiments since the on-site energy can be changed by means of a gate voltage.

Finally, we have investigated the effects of a uniaxial anisotropy field, acting on the core spin, on the YSR states. Here, both the exchange and Coulomb energies play crucial roles to determine the number of YSR states. It is important to notice that for small negative values of D [see Figs. 5(a) and 5(c)], the number of YSR states changes from three to one. Hence, keeping the values of the exchange interaction, J_{ex}, and the anisotropy, D, small and negative, a continuous variation of U/Γ should enable the observation of a change in the number of YSR states. Excitation spectra of MnPc resolved using scanning tunneling microscopy [34] also show similar changes in the properties of the YSR states. The spectral weights of the individual YSR states, moreover, show discontinuous changes across the phase transition. Future studies should involve investigations of finite temperatures and magnetic-field effects in the state emerging both inside and outside of the gap.

ACKNOWLEDGMENTS

We thank Stiftelsen Olle Engkvist Byggmästare and Vetenskapsrådet for financial support. The computations were performed on resources provided by SNIC through Uppsala Multidisciplinary Center for Advanced Computational Science (UPPMAX) under Project SNIC 2019/8-211. We thank Felix von Oppen and Katharina J. Franke for useful discussions.

[1] G. D. Scott and D. Natelson, ACS Nano **4**, 3560 (2010).
[2] A. C. Hewson, *The Kondo Problem to Heavy Fermions* (Cambridge University Press, Cambridge, 1997).
[3] P. Coleman, *Introduction to Many-Body Physics* (Cambridge University Press, Cambridge, 2015).
[4] D. Goldhaber-Gordon, H. Shtrikman, D. Mahalu, D. Abusch-Magder, U. Meirav, and M. A. Kastner, Nature (London) **391**, 156 (1998).
[5] S. M. Cronenwett, T. H. Oosterkamp, and L. P. Kouwenhoven, Science **281**, 540 (1998).
[6] J. Li, W. D. Schneider, R. Berndt, and B. Delley, Phys. Rev. Lett. **80**, 2893 (1998).
[7] N. Knorr, M. A. Schneider, L. Diekhöner, P. Wahl, and K. Kern, Phys. Rev. Lett. **88**, 096804 (2002).
[8] A. F. Otte, M. Ternes, K. von Bergmann, S. Loth, H. Brune, C. P. Lutz, C. F. Hirjibehedin, and A. J. Heinrich, Nat. Phys. **4**, 847 (2008).

[9] W. Liang, M. P. Shores, M. Bockrath, J. R. Long, and H. Park, Nature (London) **417**, 725 (2002).
[10] J. Park, A. N. Pasupathy, J. I. Goldsmith, C. Chang, Y. Yaish, J. R. Petta, M. Rinkoski, J. P. Sethna, H. D. Abruña, P. L. McEuen, and D. C. Ralph, Nature (London) **417**, 722 (2002).
[11] S. Kubatkin, A. Danilov, M. Hjort, J. Cornil, J. L. Brèdas, Ni. Stuhr-Hansen, P. Hedegøard, and T. Bjørnholm, Nature (London) **425**, 698 (2003).
[12] A. Zhao, Q. Li, L. Chen, H. Xiang, W. Wang, S. Pan, B. Wang, X. Xiao, J. Yang, J. G. Hou, and Q. Zhu, Science **309**, 1542 (2005).
[13] A. Yazdani, B. A. Jones, C. P. Lutz, M. F. Crommie, and D. M. Eigler, Science **275**, 5307 (1997).
[14] S.-H. Ji, T. Zhang, Y.-S. Fu, X. Chen, X.-C. Ma, J. Li, W.-H. Duan, J.-F. Jia, and Q.-K. Xue, Phys. Rev. Lett. **100**, 226801 (2008).
[15] S.-H. H. Ji, T. Zhang, Y.-S. S. Fu, X. Chen, J.-F. F. Jia, Q.-K. K. Xue, and X.-C. C. Ma, Appl. Phys. Lett. **96**, 073113 (2010).
[16] V. Mourik, K. Zuo, S. M. Frolov, S. R. Plissard, E. P. A. M. Bakkers, and L. P. Kouwenhoven, Science **336**, 1003 (2012).
[17] A. F. Andreev, Zh. Eksperim. i Teor. Fiz. **1228**, 46 (1964) [Sov. Phys. JETP **19**, 1228 (1964)].
[18] L. Yu, Acta Phys. Sin. **114.1**, 75 (1965).
[19] H. Shiba, Prog. Theor. Phys. **40**, 435 (1968).
[20] A. I. Rusinov, JETP Lett. **9**, 85 (1969) [Zh. Eksp. Teor. Fiz. **9**, 146 (1968)].
[21] M. I. Salkola, A. V. Balatsky, and J. R. Schrieffer, Phys. Rev. B **55**, 12648 (1997).
[22] A. Martın-Rodero and A. L. Yeyati, J. Phys.: Condens. Matter. **24**, 385303 (2012).
[23] A. Akbari, I. Eremin, and P. Thalmeier, Phys. Rev. B **81**, 014524 (2010).
[24] M. Žonda, V. Pokorný, V. Jani, and T. Novotný, Sci. Rep. **5**, 8821 (2015).
[25] M. Žonda, V. Pokorný, V. Janis, and T. Novotný, Phys. Rev. B **93**, 024523 (2016).
[26] H. Shiba, K. Satori, O. Sakai, and Y. Shimizu, Physica B **186**, 239 (1993).
[27] J. Bauer, A. Oguri, and A. C. Hewson, J. Phys.: Condens. Matter **19**, 486211 (2007).
[28] R. Žitko, Phys. B Condens. Matter **536**, 203 (2018).
[29] R. López, M.-S. Choi, and R. Aguado, Phys. Rev. B **75**, 045132 (2007).
[30] R. Žitko, M. Lee, R. López, R. Aguado, and M.-S. Choi, Phys. Rev. Lett. **105**, 116803 (2010).
[31] J. O. Island *et al.*, Phys. Rev. Lett. **118**, 117001 (2017).
[32] N. Hatter, B. W. Heinrich, M. Ruby, J. I. Pascual, and K. J. Franke, Nat. Commun. **6**, 8988 (2015).
[33] M. T. Randeria, B. E. Feldman, I. K. Drozdov, and A. Yazdani, Phys. Rev. B **93**, 161115(R) (2016).
[34] R. Žitko, O. Bodensiek, and T. Pruschke, Phys. Rev. B **83**, 054512 (2011).
[35] C. Sangregorio, T. Ohm, C. Paulsen, R. Sessoli, and D. Gatteschi, Phys. Rev. Lett. **78**, 4645 (1997).
[36] L. Thomas, F. Lionti, R. Ballou, D. Gatteschi, R. Sessoli, and B. Barbara, Nature (London) **383**, 145 (1996).
[37] B. W. Heinrich, J. I. Pascual, and K. J. Franke, Prog. Surf. Sci. **93**, 1 (2018).
[38] D. Jacob, M. Soriano, and J. J. Palacios, Phys. Rev. B **88**, 134417 (2013).
[39] K. Satori, H. Shiba, O. Sakai, and Y. Shimizu, J. Phys. Soc. Jpn. **61**, 3239 (1992).
[40] O. Sakai, Y. Shimizu, H. Shiba, and K. Satori, J. Phys. Soc. Jpn. **62**, 3181 (1993).
[41] R. Bulla, T. A. Costi, and T. Pruschke, Rev. Mod. Phys. **80**, 395 (2008).
[42] T. Hecht, A. Weichselbaum, J. von Delft, and R. Bulla, J. Phys.: Condens. Matter **20**, 275213 (2008).
[43] V. Meden, J. Phys. Condens. Matter **31**, 163001 (2019).
[44] R. Žitko, Proc. SPIE **10732**, 107321N (2018).
[45] A. V. Rozhkov and D. P. Arovas, Phys. Rev. B **62**, 6687 (2000).
[46] Y. Tanaka, A. Oguri, and A. C. Hewson, New J. Phys. **9**, 115 (2007).